5th Conference on Aerospace Materials, Processes, and Environmental Technology (AMPET)
September 16-18, 2002
Von Braun Center
Huntsville, Alabama

Hydrogen Permeability of a Polymer Based Composite Tank Material Under Tetra-Axial Strain

Eric H Stokes
Southern Research Institute
Birmingham, AL

INTRODUCTION

In order to increase the performance of future expendable and reusable launch vehicles and reduce per-pound payload launch costs, weight reductions have been sought in vehicle components. Historically, the cryogenic propellant tanks for launch vehicles have been constructed from metal. These are some of the largest structural components in the vehicle and contribute significantly to the vehicles total dry weight. A successful replacement material will be conformable, have a high strength to weight ratio, and have a low gas-permeability to the cryogens being stored, i.e., oxygen and hydrogen. Polymer-based composites are likely candidates to fill this role. Polymer and polymer-based composites in general are known to have acceptable gas permeation properties in their as-cured state.[1] The use of polymer-based composites for this application has been proposed for some time.[2] Some successes have been reported with oxygen[3], but other than the DC-XA experience,[4,5] those with hydrogen have been limited. The primary reason for this has been the small molecular diameter of hydrogen, the lower temperatures of the liquid, and that the composite materials examined to date have all been susceptible to microcrack formation in response to the thermal-mechanical cycles experienced in the use-environment. There have been numerous accounts of composite materials with reported acceptable resistance to the formation of microcracks when exposed to various mechanical and/or thermal cycles. However, virtually all of these studies have employed uniaxial loads and there has been no discussion or empirical evidence pertaining to how these loads relate to the biaxial state of stress in the material in its use environment. Furthermore, many of these studies have suffered from a lack of instrument sensitivity in detecting hydrogen permeability, no standards, insufficient documentation of test conditions, testing of cycled materials in their unload state, and/or false assumptions about the nature of the microcracks in the material. This paper documents the results of hydrogen permeability testing on a Bis-maleimide (BMI) based graphite fiber composite material under a variety of tetra-axial strain states.

MATERIALS AND METHODS

Five flat 12 inch by 12 inch by roughly 0.055 inch polymer matrix graphite fiber composite panels were delivered for testing. All of the panels were constructed from ten plys of 5½ mil uniaxial graphite fiber tape. The polymer matrix for the panels was a BMI resin. Yarns were oriented [90/60/90/-60/0]s, i.e., [90/+60/90/-60/0/0/-60/90/+60/90], to simulate the architecture needed for a cylindrical tank requiring a 2:1 ratio of mechanical properties. Four of the five panels were delivered in there as-processed state. Panel 3 was delivered preconditioned through 2500 uniaxial 0 to 5000 micro-strain tensile cycles in the 0° direction followed by the same in the 90° direction. The cycling was done at liquid hydrogen temperatures. One nine-inch and up to four 2.1 inch diameter permeability specimens were machined from each test panel. Eight uniformly distributed slots were machined radially from various concentric diameters to the outer diameter of the nine inch specimen producing eight pull-tabs used to apply the areal tensile strain in the specimen. Care was taken to avoid contamination of the surface of the specimen during machining and subsequent handling. Eight uniaxial strain gages were adhesive attached every 45° on a 3.25 by 3.75 inch concentric annulus around the specimen. One strain gage was mounted on the centerline of each pull-tab. Two type E thermocouples were adhesively attached to the reverse side of the specimen 180° apart on a 4.5 inch concentric circle with the specimen.

The gas permeability facility utilized in this study was calibrated using NIST SRM 1470 as described in ASTM D 1434 - 82 (Reapproved 1997). Room temperature gas permeability was measured on the specimen in the thickness direction. A circular gage section with a diameter of 1.5 or 1.8 inches at the center of each specimen was the material employed to measure the material's permeability under strain. To run the test, the specimen was placed in the facility. A sealing gasket was placed on the downstream and upstream halves of the facility and the two halves were mated. A compressive force was applied to the two halves of the facility through stainless steel 1.0-inch diameter balls that insured the alignment and even distribution of force on the specimen seals. A dynamic vacuum was applied to the upstream, downstream, and edges of the specimen overnight or until the specimen ceased to outgas. The downstream valve between the vacuum pump and transducer was then closed. After a sufficient record was obtained at these settings, hydrogen gas at a fixed pressure was applied to the upstream surface from a high pressure, high purity (5.5) hydrogen gas source. The increase in pressure downstream as a function of time was converted to a mass flow rate using the ideal gas equation. The mass flow rate was corrected for background outgassing from the specimen. The permeability in mol*m/m^2*s*Pa was calculated from the mass flow rate, specimen dimensions, and differential gas pressure across the specimen.

For measurements under tetra-axial strain the strain gages on the specimen and load cells on the facility were calibrated and zeroed prior to specimen installation. The specimen was placed in the loading facility. Each pull-tab of the specimen was aligned with one of the eight grips on the loading facility. The tensile load on each pull-tab was increased until the predetermined strain in each of the eight directions was obtained. All permeability testing of specimens was done at uniform levels of strain in the eight in-plane directions within the material. A record of the final strain in each of the eight directions was obtained. In some cases at elevated strain levels strain gages were lost due to surface cracks that developed in the materials under the gages. In those cases, a plot of load versus strain was constructed for the strain gage that failed and strains were estimated by extrapolating the load vs. strain data to the higher level of strain of interest. Loads were then calculated and applied that provided the pre-selected strain level. The permeability facility was positioned in place over the center of the specimen for measurement of the specimen's permeability. Strain levels were monitored during the sealing process to insure that no bending stresses are introduced to the specimen. The permeability facility has the capability of adjusting specimen orientation in the facility to relieve any parasitic stress states that may develop during the sealing process. The specimen orientation in the facility was adjusted until the measured strain in each of the eight directions of the specimen were equal to the strain in the specimen prior to sealing. The permeability of the material was then measured as stated above.

RESULTS

The hydrogen permeability data for the unstrained material in its as-processed state at room temperature (RT) are shown for two 2.1" diameter specimens taken from Panel 1in Figure 1. The nine-inch specimen from this panel, S1, was taken to 2500 micro-strain (με) in 500 με increments at room temperature with no significant increase in permeability. Upon reaching 2500 με the specimen exhibited several audible micro-failures and the gage at 135° failed (infinite resistance across the gage). A couple of small cracks were observed in the visible part of the gage section upon inspection of the specimen while under strain. The cracks were not visible once the strain was removed. Subsequent permeability measurements indicated the failures were surface structures that did not extend contiguously through the thickness of the material.

The nine-inch specimen from Panel 2, S2, was taken to 2500 με in 500 με increments with a significant increase in lateral flow upon reaching 2500 με. The specimen did not exhibit any audible sounds upon reaching 2500 and all gages were functioning. Upon removing the strain the lateral flow returned to as-processed levels. When the specimen was taken down to LN2 temperature and strain applied, the 0 and 180° gages were lost (infinite resistance) between 1500 and 2000 με. Furthermore, background gas flow into the downstream chamber increased dramatically indicating that the surface layers of the specimen were developing a significant system of micro-cracks. Between 2000 and 2500 με, the four off-axis gages, i.e., 45, 135, 225, and 315°, were lost. Only the 90 and 270° gages continued to function out to 2500 με. Post-test inspection of the gages indicated the gages were broke in tension probably due to a crack crossing the gage element. The damaged gages were replaced and the specimen was then taken down to LHe temperature. The high background levels of flow were due to surface cracks, which did not form contiguous paths through the thickness of the material. Following the cryo testing at

2500 με, the strain in the specimen was removed, the specimen was returned to RT, and the permeability measured. The background levels of flow returned to as-processed levels. Figure 1 shows the permeability as a

Figure 1. Permeability of IM7/BMI (Panels 1 & 2)
as a Function of Axisymmetric Strain State

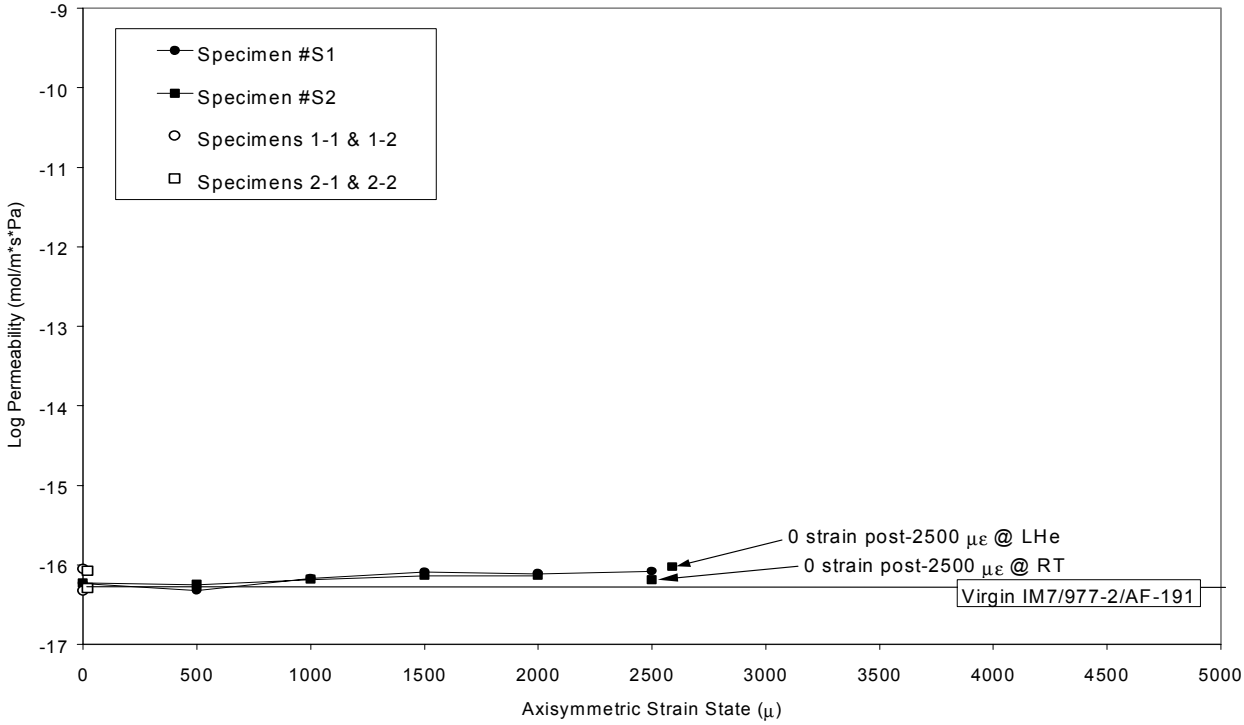

function of the applied tetra-axial strain for this specimen as well as two additional RT as-processed measurements from this panel.

The nine-inch diameter specimen from Panel 4, S4, was subjected to a number of modifications and load cycles. In addition, eight load cells were added to the permeability/strain facility prior to the testing of S4. Figure 2

Figure 2. Permeability of IM7/BMI (Panel 4)
as a Function of Axisymmetric Strain State

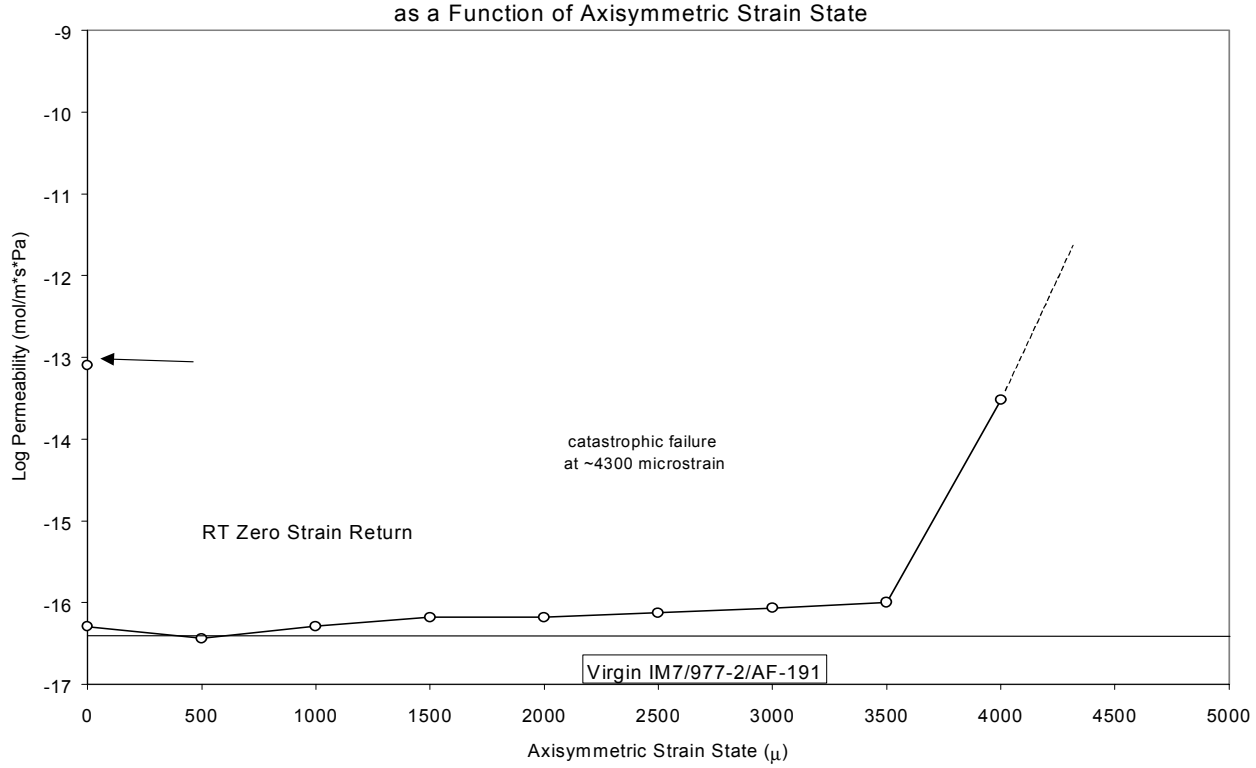

summarizes the permeability data for this specimen and compares it to the virgin unstrained quasi-isotropic IM7/977-2/AF-191.[6] The strain in specimen S4 was incrementally increased at room temperature. Small but steady increases in permeability (500 με excepted) were measured out to 3500 με. At 4000 με the specimen exhibited a large increase in hydrogen permeability. At approximately 4300 με the specimen catastrophically failed. Three of the eight pull-tabs (90, 135, and 180°) tore off at the inner most bolt circle. Hydrogen permeability of the specimen after it was removed from the loading facility was higher than the value obtained at 4000 με but lower than the anticipated permeability of the material at the point of failure (4300 με) by extrapolation of the log permeability vs. strain data (fig. 2).

Figure 3. Permeability of IM7/BMI (Panel 5) as a Function of Axisymmetric Strain State

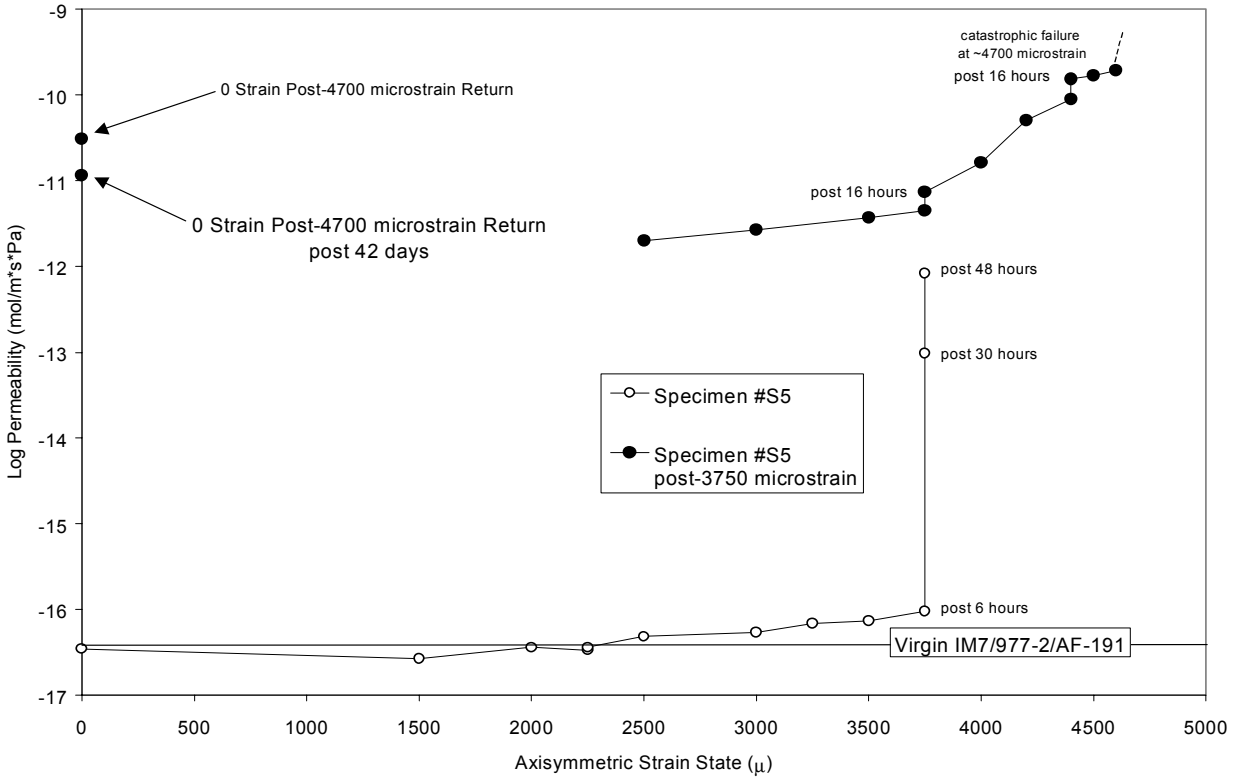

The tetra-axial strain in specimen S5 was likewise incrementally increased at room temperature. Small but steady increases in permeability were observed out to 3750 με. Smaller steps in strain were taken above 3000 με in order to more clearly observe the point where contiguous micro-crack development begins. At 3750 με the specimen exhibited a relatively small increase in hydrogen permeability consistent with the increases seen at lower strain levels. However, after 30 hours at 3750 με the specimen's permeability to hydrogen jumped by nearly three orders of magnitude over its permeability after 6 hours. After an additional 18 hours, the material's permeability to hydrogen increased by another order of magnitude. As might be anticipated, time at any elevated strain level is a significant factor in the development of a network of contiguous microcracks and rise in the material's permeability to hydrogen. A related behavior was also seen during off-loading when after dropping to some load level the strain, particularly in the 90 and 270° directions, was observed to creep to lower levels as a function of time. As with S4, significant surface cracks were detected upon reaching 2500 με. Figure 3 summarizes the permeability data for this specimen.

Figure 4 shows the load versus strain data for Run 2 Loading 1 (R2L1) of specimen S5. A curve is drawn through the 90° data showing the approximate shape of the curve describing this data. As can be seen in this figure the 90, 135, 180, and 315° directions exhibited strain offsets in the load versus strain data as low as 1500 με. Following the strain offset the slope of the load versus strain data generally became steeper indicating that a larger load

differential was required to cause a fixed incremental change in measured strain. This would be consistent with the formation of surface cracks that might partially de-couple the surface from the underlying material.

Figure 4. Mechanical Response of Specimen S5 to Tetra-Axial Tensile Loads
(Run 2 Loading 1)

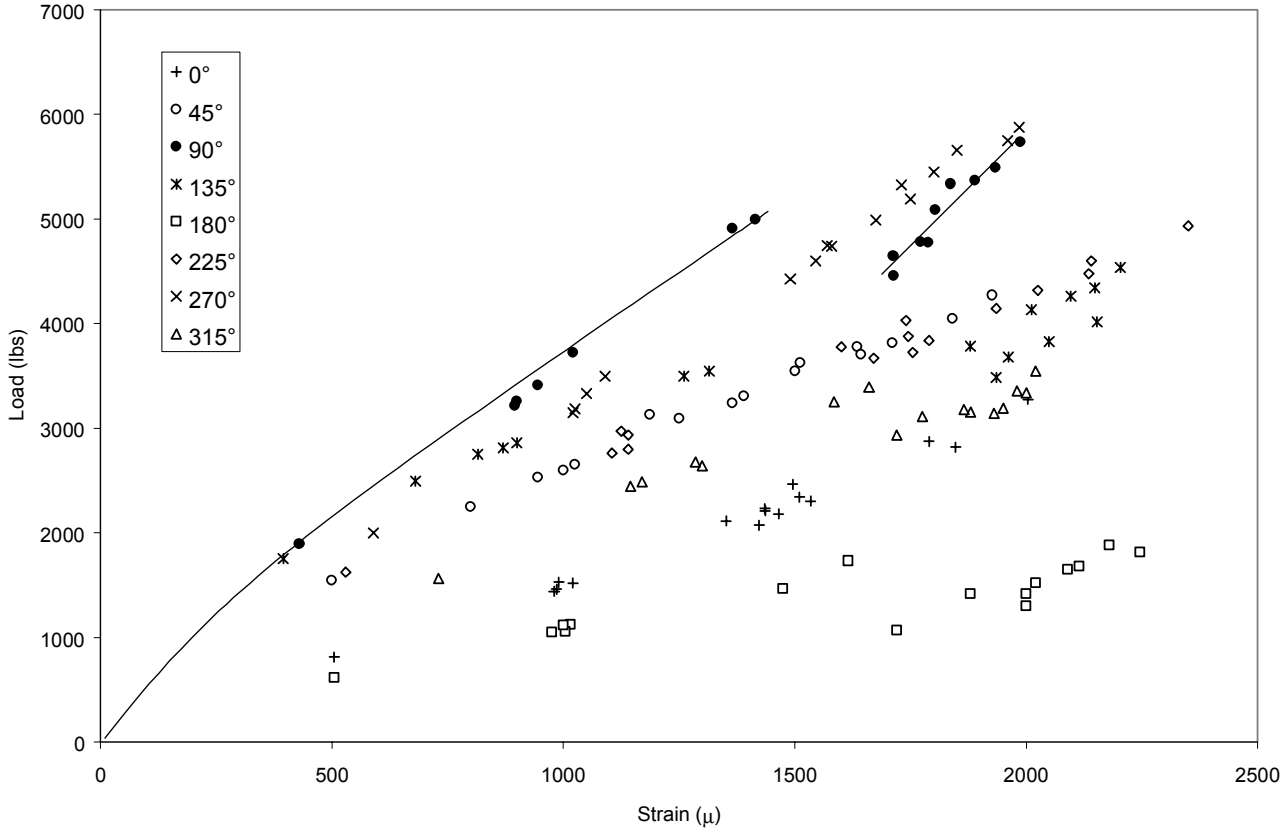

Permeability measurements were made following most runs after loads were removed. It was observed that these unstrained return values were generally higher than the values obtained prior to the application of load. Similar findings have been observed previously on other composite materials.[7,8] However, this response appears to be material specific.[9] Subsequent measurements of permeability on the unloaded specimens revealed that the permeability of the materials generally decreased with time and in some cases returned to pre-strained levels.[9] Figure 5 shows the loading and unloading data for Run 3 Loading 1 (R3L1) of specimen S5. There was a strong hysteresis exhibited by the material during offloading. This could explain the initial higher zero strain return permeability data that over time returns to the pre-strained levels. It is not clear at this point what is responsible for the time dependent strain recovery and changes in permeability during off-loading. However, movement of the softer cured resin into existing porosity under the influence of the residual stress in the graphite fibers during off-loading of the composite is suspected.

Figure 6 shows the load versus strain data for Run 3 Loading 2 (R3L2) of specimen S5. Above 3250 με the 90° data exhibited several large strain offsets. This was accompanied by the appearance of visible evenly spaced cracks spaced about 50 to 60 mils apart running in the 90-270° direction. The appearance of the cracks also coincided with the dramatic rise in hydrogen permeability measured at 3750 με (fig. 3). In addition, a strain offset was seen in the 45° direction above 3750 με.

Figure 7 shows a comparison of 90° data from a series of S5 loadings. The relatively small strain offset at 1500 με is visible with R2L1, as are the much larger strain offsets associated with R3L2. Contiguous through thickness micro-cracks had formed by the time S5 was offloaded from R3L2 as evidenced by the gas permeability data (fig.

Figure 5. Mechanical Response of Specimen S5 to Tetra-Axial Tensile Loads
(Run 3 Loading 1)

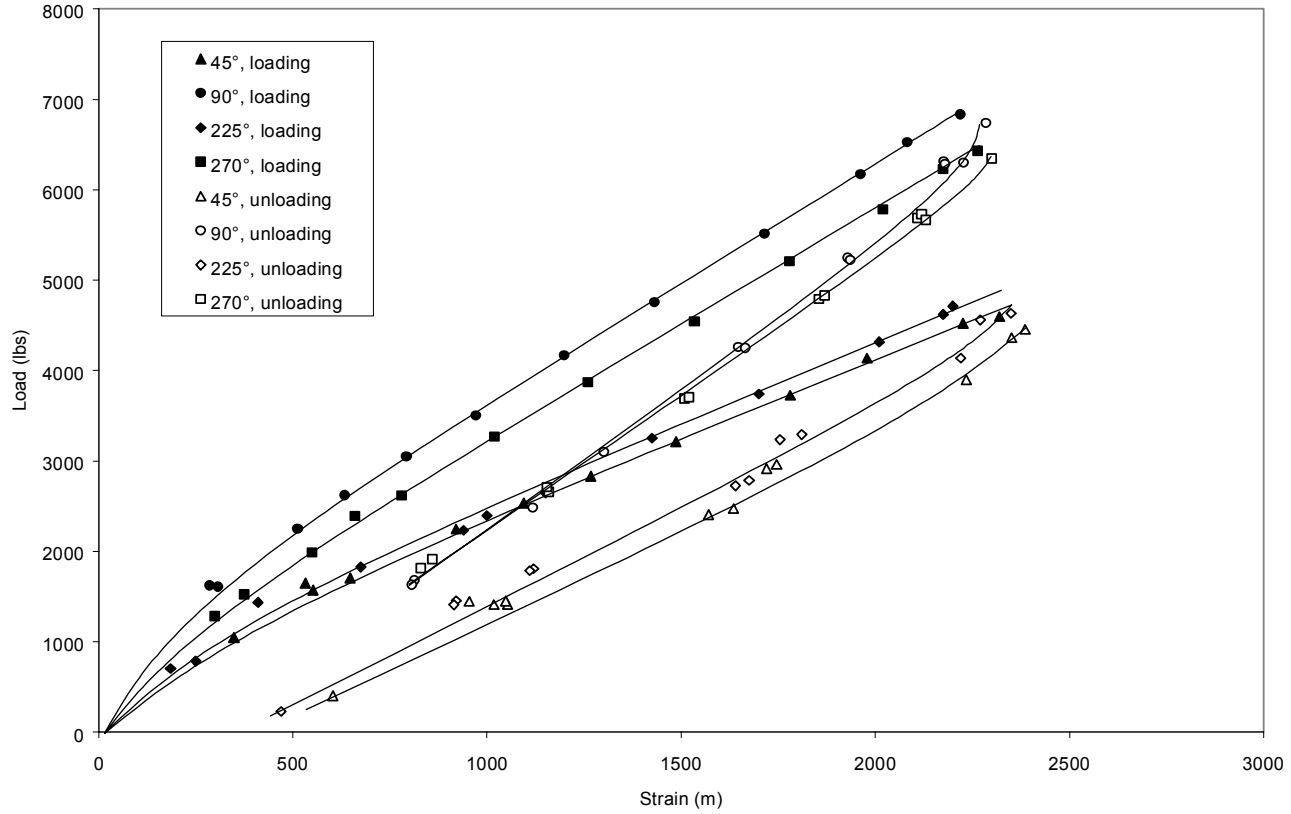

Figure 6. Mechanical Response of Specimen S5 to Tetra-Axial Tensile Loads
(Run 3 Loading 2)

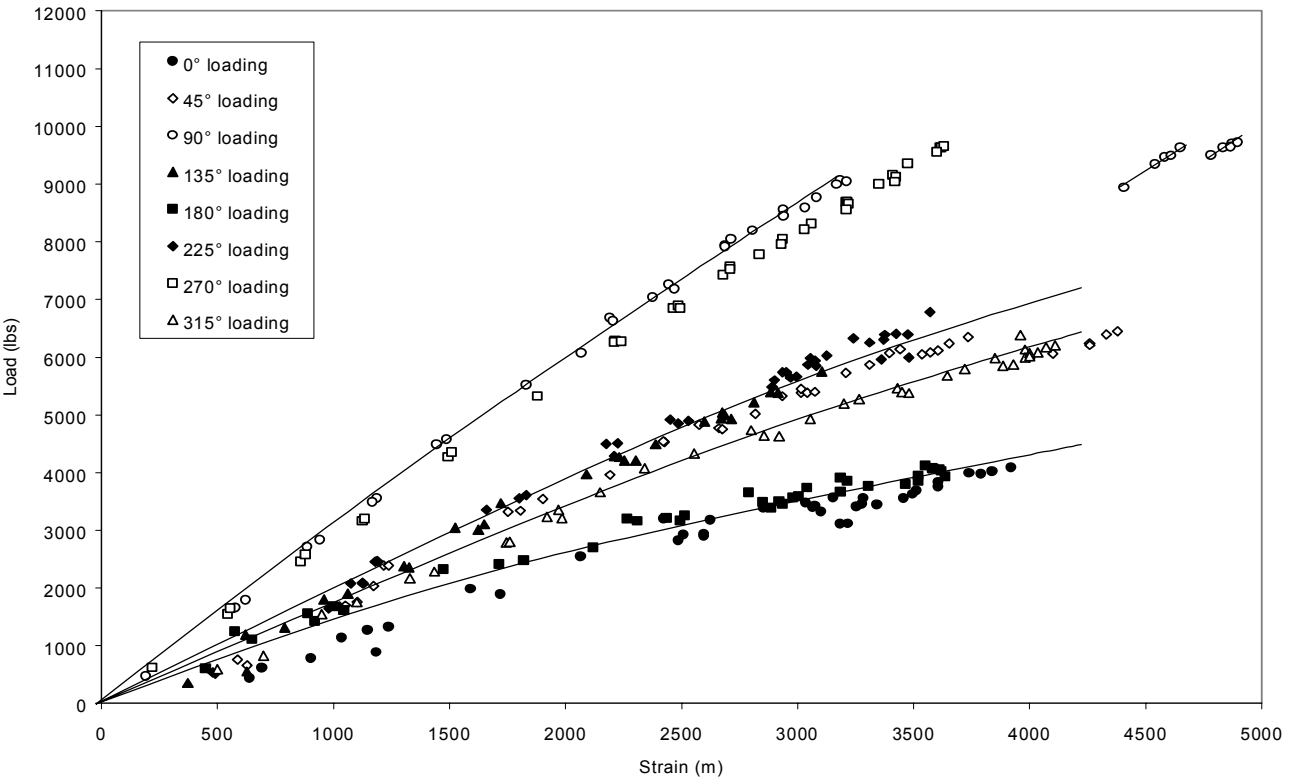

Figure 7. Mechanical Response of Specimen S5 to Tetra-Axial Tensile Loads
(Comparison of 90° Response)

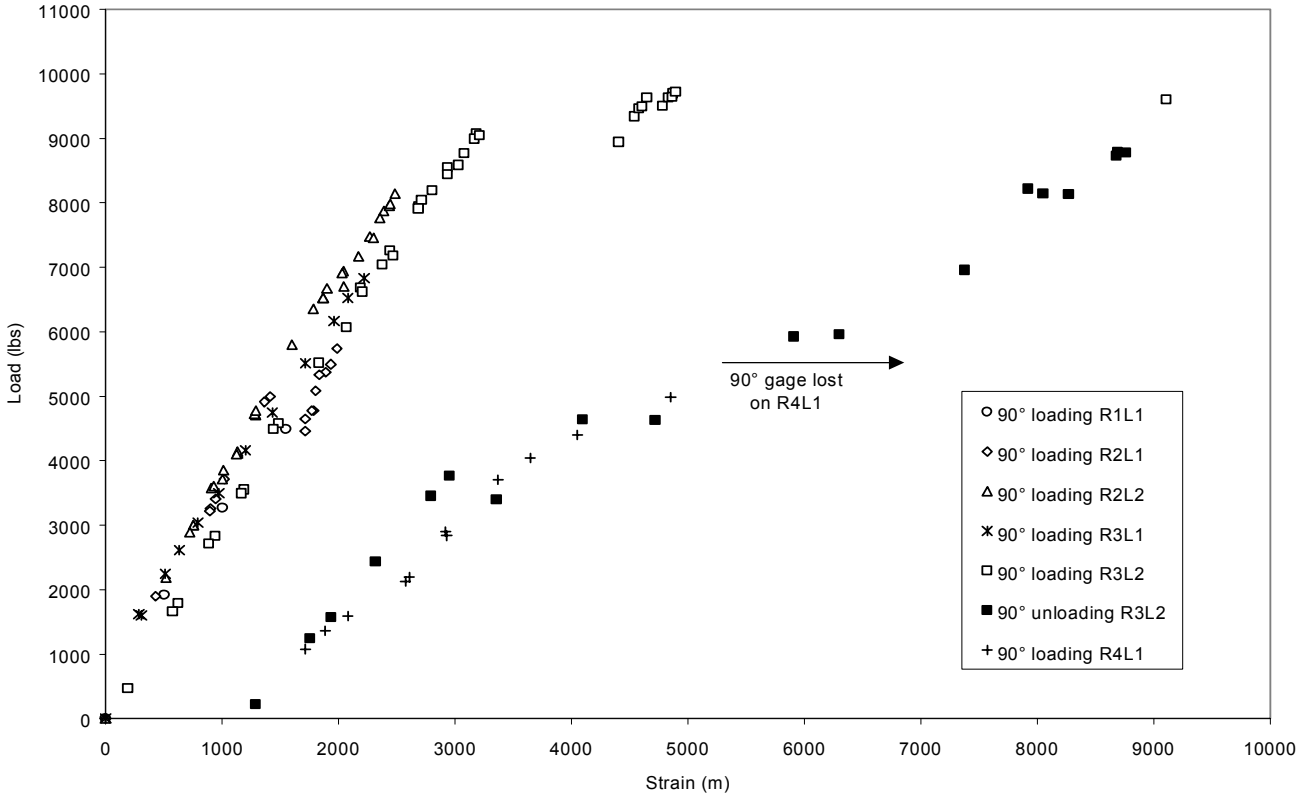

3). During loading in the subsequent run, R4L1, the specimen exhibited load versus strain behavior that followed the offloading curve of the previous run closely. This varied with the runs that followed the strain offsets prior to contiguous micro-crack formation indicating a significant change in tetra-axial tensile modulus with the development of through thickness cracks.

Figure 8 compares the hydrogen permeability data for the four specimens of virgin IM7/BMI (S1, S2, S4, & S5), one preconditioned IM7/BMI (S3), and virgin unstrained quasi-isotropic IM7/977-2/AF-191 (X-33).[6] Strain offsets in load versus strain data for the two specimens, S4 and S5, indicated that localized failures are occurring as low as 1500 με. These offsets are probably the result of the development of surface micro-cracks under the attached strain gages but indicate that the material is undergoing crack initiation as low as 1500 με under tetra-axial loading conditions. Widespread micro-cracking of the surface plies (90-270°) begins between 2500 and 3000 με at room temperature under uniform in-plane strain. Evidence for this can be seen in the high background flow rates seen with all four virgin specimens. These high backgrounds generally started at around 2500 με and progressively increased with applied strain. Strain measurements were made on the upstream surface of the specimen whereas flow measurements were made on the downstream surface so these two observations indicate that both surfaces are developing a system of micro-cracks at relatively low strain levels. In further support of these observations, an explosive gas detector was kept in close proximity to the test facility during all testing. It would routinely go off at around 2500 με when permeability testing was initiated and high-pressure hydrogen gas was being applied to the upstream surface of the specimen. This further supports the findings that surface cracks from both surfaces of the material were forming at comparatively low strain levels. However, through thickness flows were essentially constant out to much higher strain levels. The internal plies begin to micro-crack between 3500 and 4000 με at room temperature with uniform in-plane strain. These four observations would imply that crack initiation, with this material in the absence of any bending loads, begins at both surfaces and progressively extends toward the center of the panel.

Figure 8. Permeability of IM7/BMI as a Function of Axisymmetric Strain State

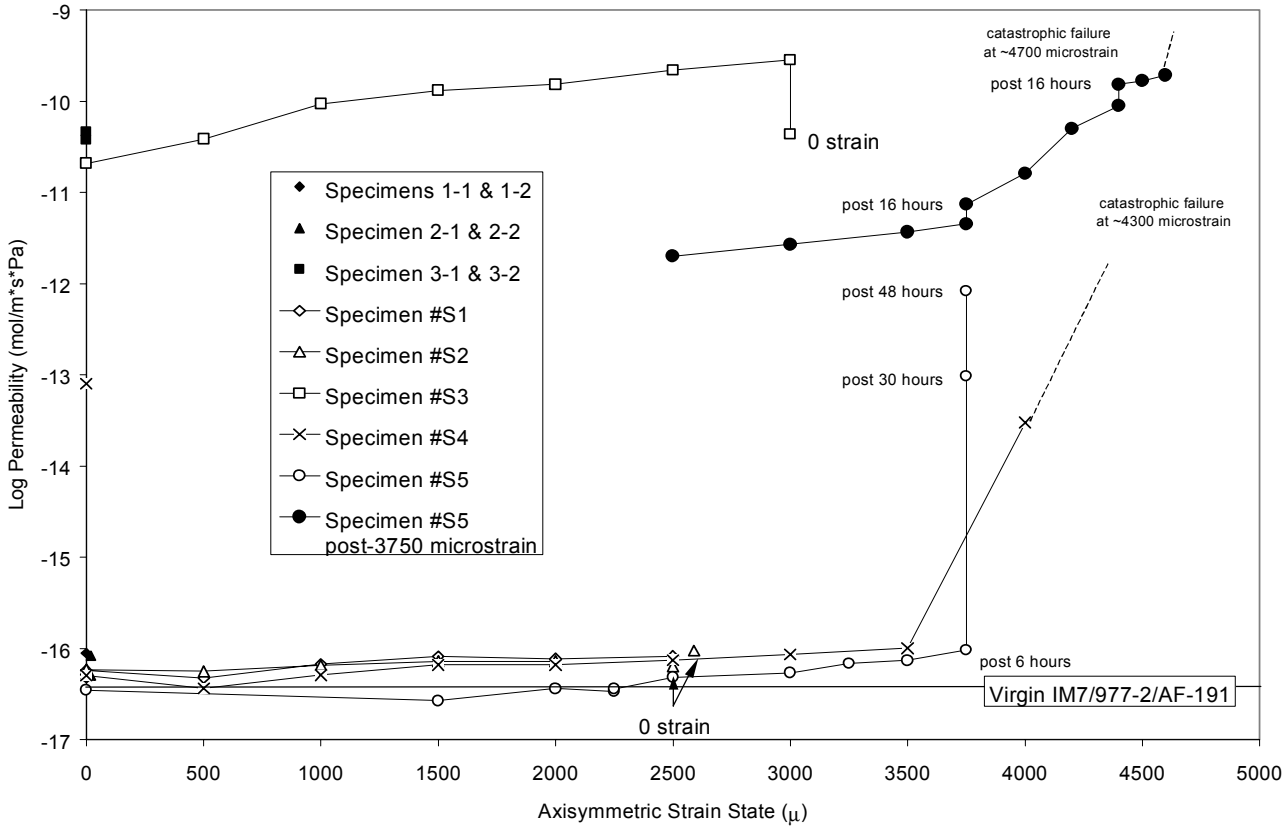

Figure 8 summarizes the effects of in-plane tetra-axial tensile strain on the hydrogen permeability of the Panel 3 material, S3. The unstrained preconditioned material had a permeability to hydrogen that was roughly 6 order of magnitude higher than the as-cured non-preconditioned material. The material exhibited consistent increases in hydrogen permeability with strain out to 3000 micro-strain, the maximum strain applied. There was greater than an order of magnitude increase in permeability between the initial unstrained and 3000 micro-strained states. Upon releasing the tetra-axial tensile load on the specimen following the application of 3000 micro-strain the material returned to the same permeability that it exhibited in its initial unstrained state.

Figure 9. Photomicrograph of 0/180° Slice (top) and 90/270° Slice (bottom) from Panel #3 (Preconditioned)

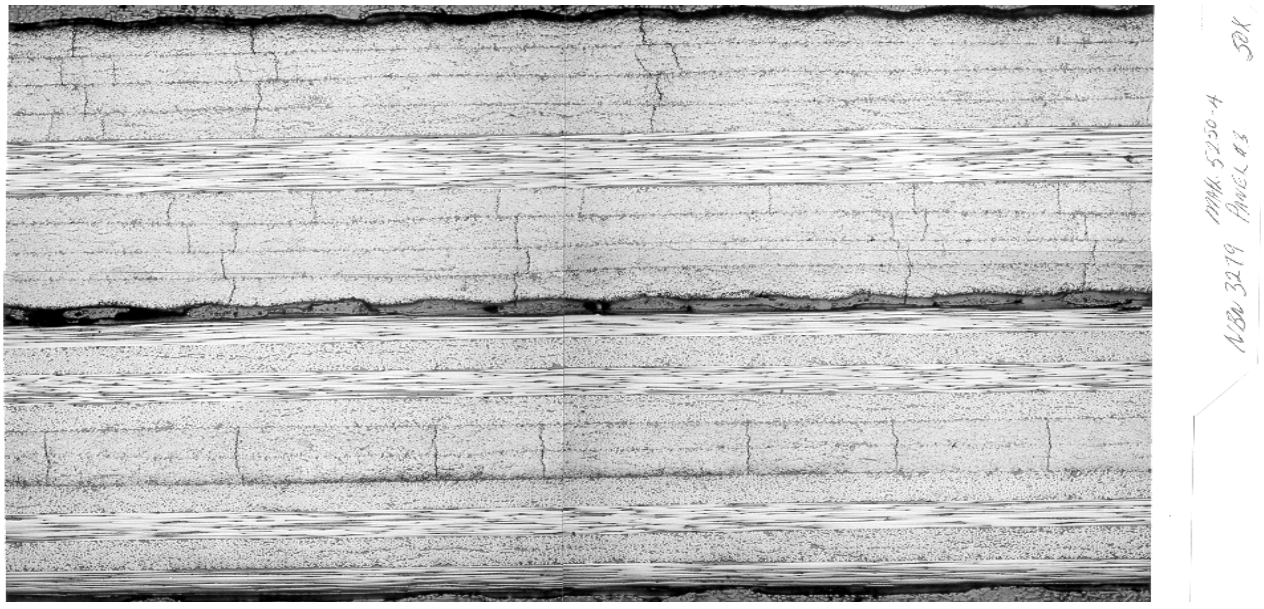

Figure 10. Crack Density by Ply for Five IM7 Based Preconditioned Composites

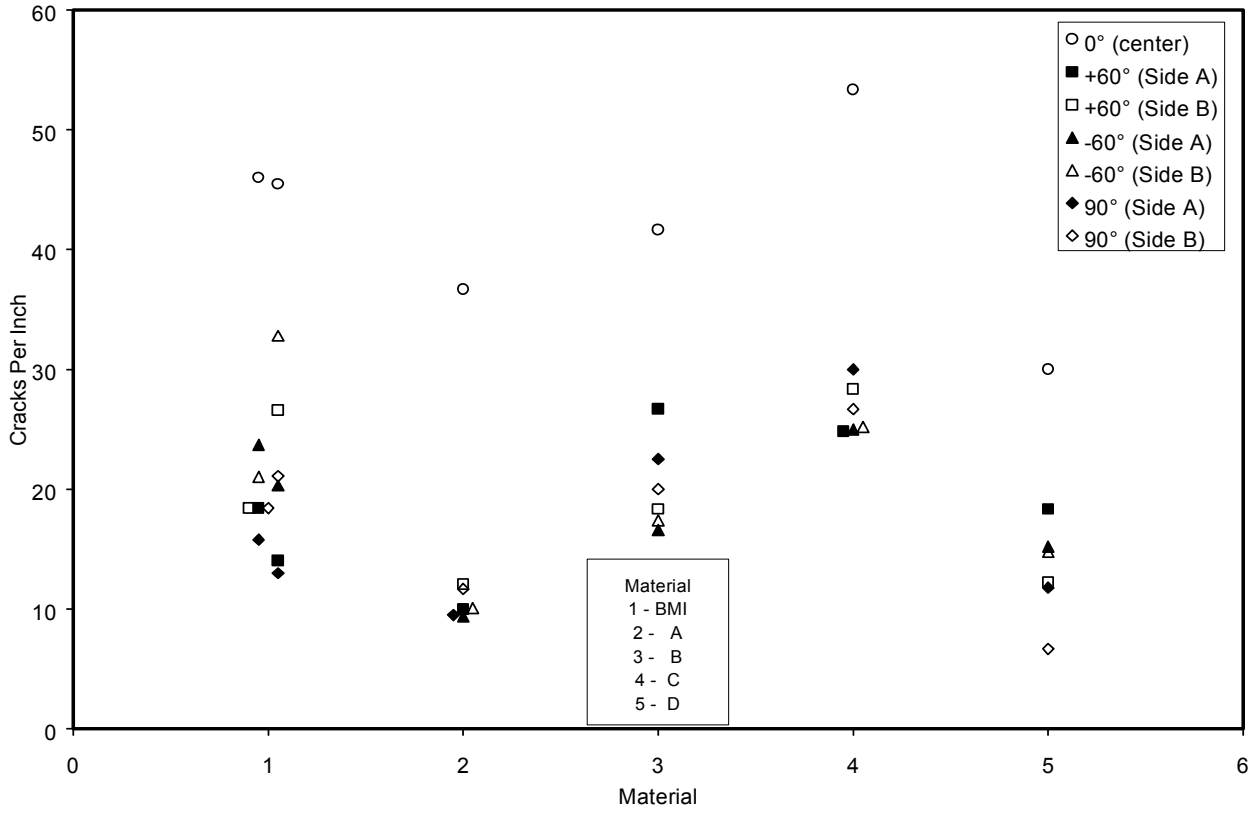

Figure 9 shows a photomicrograph of two stacked cross-sections through preconditioned Panel #3. The yarn architecture of the panel can be seen as well as a large number of cracks that run in the through thickness direction. The number of cracks per inch (crack density) varied from ply to ply. The plies lying in the center of the composite (0° plies) had the largest number of cracks per inch followed by the plies (-60°) that were adjacent to the center plies.

Figure 10 is a graph of the observed crack densities of five different preconditioned composite materials with the same yarn architecture by ply orientation. As can be seen in this graph the center 0° plies consistently had the highest crack densities. The adjacent –60° plies in all cases except the BMI material had crack densities that were similar to the other non-zero degree plies. In the case of the BMI material crack densities for the adjacent –60° plies was generally higher than the other non-zero degree plies.

CONCLUSIONS

1. Failure initiation for the BMI material under uniform in-plane strain is from the exposed surfaces and progresses toward the center of the material. In addition to the evidence of this from permeability testing, a post-test microscopic examination of the top and bottom four plies of the material indicate that wider cracks can be seen at the surface (90° plies) than in depth.
2. There is evidence that localized failures may be occurring in surface plies of the BMI material as low as 1500 micro-strain at room temperature with uniform tetra-axial in-plane strain.
3. Widespread micro-cracking of the surface plies of the BMI material begins between 2500 and 3000 micro-strain at room temperature under uniform tetra-axial in-plane strain.
4. A contiguous through-thickness crack system begins to form in the BMI material between 3500 and 4000 micro-strain at room temperature under uniform tetra-axial in-plane strain. It's unclear whether the 0 or –60° plies are the last to form microcracks. Intuitively, one might anticipate that the 0° plies would be the last to crack since they are mechanically the most supported and furthest from crack intiation. Microscopic evidence seems to

suggest the –60° (adjacent to the 0° plies) layers are the least open in the unstrained state. However, these plies are adjacent to the 0° plies, which would tend to close these cracks up on off-loading. Numerically, the –60° plies had the second highest crack density (cracks/inch) next to the 0° plies.

5. In addition to the material's strain level and temperature, permeability is a time dependent parameter for many of these the materials at RT and needs to be defined as such. Creep is an accepted phenomenon, particularly with polymers at elevated temperature or high loads. It's not clear how applicable it would be in a material that is generally mechanically loaded at cryogenic temperatures.

6. Catastrophic failure of the BMI material occurs somewhere above 4600 micro-strain at room temperature under uniform in-plane strain. Given the observed development of a significant crack system at 3750 micro-strain, the strain-to-failure of the material under axisymmetric loading can not be much greater than 5000 microstrain, which would be significantly less than that found when the material is unidirectional loaded.

7. For the BMI material that was not initially microcracked, strain was the first order variable with respect to the material's permeability.

8. For materials that already had a well-developed crack system, temperature was the first order variable with respect to the material's permeability. However, in most cases the applied strains were low relative to the anticipated strain-to-failure of these materials. Conversely, the general response of these materials to strain was highest at low strain levels suggesting that the changes observed out to 1500 με included the predominate response of the materials to changes in strain.[9,10]

9. The as-processed BMI material exhibited a time dependent sealing mechanism at room temperature after returning to an unstrained state from a series of microcrack inducing tetra-axial strain levels. A hysteresis effect between loading and unloading in load vs. strain curves generally accompanied this phenomenon. A similar mechanism was seen with some of the other preconditioned materials but more data is needed before definitive conclusions can be drawn with respect to these materials.

Acknowledgements

The author wishes to thank The Boeing Company, Huntington Beach, CA and in particular Jeff Eichinger, Mike Robinson and Scott Johnson for supporting this effort. This work was conducted with funds from NASA's SLI Program.

References

[1]Stokes, E. H., "Hydrogen Permeability of Polymers and Polymer-Based Composites," SRI-ENG-01-36-A392, July 2001, 72 p.

[2]Feldman, A., Giguere, A. J., Stang, D. A., "Design Application Of High-Modulus Filament-Wound Composites To Aerospace Propellant And Pressurization Tanks," In: MATERIALS AND PROCESSES FOR THE 70'S, SAMPE National Symposium And Exhibition, 15TH, Los Angeles, Calif, Apr. 29-May 1, 1969, Proceedings, pp. 151-161/A69-35501, 1969.

[3]Black, S., "X-34 Composite Liquid Oxygen Tank a First," High-Performance Composites, 2000(7-8):52-54, 2000.

[4]Nettles, A.T., "Permeability Testing of Composite Material and Adhesive Bonds for the DC-XA Composite Feedline Program," NASA TM 108483, March 1995.

[5] Cast, J., "Delta Clipper Rolls Out; Flight Tests to Begin in May," NASA Press Release #96-51, March 15, 1996. http://www.hq.nasa.gov/office/pao/History/x-33/nasa-96-51.htm

[6]Stokes, E. H., "Hydrogen Permeability Of Graphite Epoxy Composite Hydrogen Tank Materials As A Function Of Temperature And Bi-Axial Strain State," SRI-ENG-00-06-8657.22, February 2000, 253 p.

[7]Stokes, E. H., "Hydrogen Permeability at Room and Cryogenic Temperature of a Graphite Epoxy Composite Tank Panel Under Bi-Axial Strain," SRI-ENG-00-32-A194.01, December 2000, 33 p.

[8]Stokes, E. H., SRI-ENG-01-56-A435.0, November, 2001, 35 p.

[9]Stokes, E. H., "Hydrogen Permeability of Graphite Fiber Composite Hydrogen Tank Materials as a Function of Temperature and Tetra-Axial Strain State," SRI-ENG-02-17-A439, July 2002, 109 p.

[10]Eichinger, J. and Stokes, E.H., "Permeability Of Composite Hydrogen Tank Materials as a Function of Temperature and Strain State," In: Proceedings 44th AIAA/ASME/ASCE/AHS/ASC Structure, Structural Dynamics, and Material Conference, Special Session: Cryogenic Propellant Tanks and Integrated Structures for a Next Generation Reusable Launch Vehicle, April 7-10, 2003, Norfolk, VA, in press.